

Expression cloning of rat renal $\text{Na}^+/\text{SO}_4^{2-}$ cotransport

DANIEL MARKOVICH, JUDITH FORGO, GERTI STANGE, JÜRIG BIBER, AND HEINI MURER*

Institute of Physiology, University of Zürich, Winterthurerstrasse 190, 8057 Zürich, Switzerland

Communicated by Robert W. Berliner, May 25, 1993

ABSTRACT Injection of rat kidney cortex mRNA into *Xenopus laevis* oocytes leads to a stimulation of Na^+ -dependent SO_4^{2-} uptake. Based on this information, we have isolated from a corresponding library a cDNA (NaSi-1) that is most likely related to a $\text{Na}^+/\text{SO}_4^{2-}$ cotransport system. NaSi-1 cRNA leads in a time- and dose-dependent manner to specific stimulation of Na^+ -dependent SO_4^{2-} uptake in oocytes. The apparent affinity constants of the NaSi-1 cRNA-expressed transport resemble those of $\text{Na}^+/\text{SO}_4^{2-}$ cotransport in brush-border membrane. The NaSi-1 cDNA contains 2239 bp [including a poly(A) tail] and encodes a protein of 595 amino acids (66.05 kDa); the hydropathy profile suggests at least eight membrane-spanning regions. *In vitro* translation of NaSi-1 cRNA results in a protein of the expected size and suggests glycosylation. Northern blot analysis shows signals of 2.3 and 2.9 kb in kidney (more abundant in cortex than in papilla/medulla) and in mucosa of small intestine of rats. The above data indicate that we have structurally identified a membrane protein involved in renal and small-intestinal brush-border membrane $\text{Na}^+/\text{SO}_4^{2-}$ cotransport.

The mammalian kidney plays an important role in the maintenance of SO_4^{2-} homeostasis. Urinary excretion of SO_4^{2-} is $\approx 10\%$ of the filtered load; the tubular reabsorption is mainly achieved by a Na^+ -dependent (secondary-active) transport mechanism located in the proximal tubules. Studies with brush-border membrane vesicles isolated from kidney cortex of a variety of animal species have identified a $\text{Na}^+/\text{SO}_4^{2-}$ cotransport system, with an apparent K_m for Na^+ between 25 and 50 mM and a Hill coefficient exceeding unity; the apparent K_m for SO_4^{2-} is between 0.5 and 1 mM. $\text{Na}^+/\text{SO}_4^{2-}$ cotransport interacts with other oxyanions such as thiosulfate, but not with phosphate (for review see ref. 1; see also refs. 2–8). Small-intestinal brush-border membranes also contain a $\text{Na}^+/\text{SO}_4^{2-}$ cotransport system; this transport system has properties similar to those of the renal and has its highest activity in ileal brush-border membranes (e.g., ref. 3). In the proximal tubule, transcellular transport (reabsorption) is completed at the basolateral cell surface, most likely by an anion-exchange mechanism shared by bicarbonate and hydroxyl ions as well as by a variety of organic anions (1, 2).

$\text{Na}^+/\text{SO}_4^{2-}$ cotransport might be an ideal target mechanism for physiological regulation of renal SO_4^{2-} reabsorption, similar to brush-border membrane Na^+/P_i cotransport (1, 9). Glucocorticoid treatment led to a reduction in chicken renal brush-border $\text{Na}^+/\text{SO}_4^{2-}$ cotransport activity (8), whereas treatment with thyroid hormone produced an increased $\text{Na}^+/\text{SO}_4^{2-}$ cotransport activity in mouse renal brush-border membranes (10). Dietary sulfate supply also seems to modulate renal brush-border membrane $\text{Na}^+/\text{SO}_4^{2-}$ cotransport activity (11, 12).

Until now, only a few of the renal brush-border membrane $\text{Na}^+/\text{solute}$ cotransport systems have been structurally identified [e.g., $\text{Na}^+/\text{D-glucose}$ cotransport (13, 14) Na^+/P_i co-

transport (15, 16)]. In addition to obtaining structure–function information, a molecular identification of such transport systems is a mandatory prerequisite for future studies on the cellular mechanisms involved in regulatory control of proximal-tubular solute transport. Here we describe the expression cloning of rat renal cortex $\text{Na}^+/\text{SO}_4^{2-}$ cotransport, using *Xenopus laevis* oocytes. The identified cDNA (NaSi-1) encodes a protein of ≈ 66 kDa with at least eight putative transmembrane regions.† Kinetic properties of the expressed uptake, as well as tissue distribution of NaSi-1-related mRNAs, strongly suggest that NaSi-1 is closely related to $\text{Na}^+/\text{SO}_4^{2-}$ cotransport activity of brush-border membranes in renal proximal tubules and small intestine.

EXPERIMENTAL PROCEDURES

***Xenopus laevis* Oocytes and Transport Assay.** Methods for handling of oocytes and the assay for transport have been described (15–18). Oocytes were injected with 50 nl of water without cRNA or with cRNA at 0.005–1 $\mu\text{g}/\mu\text{l}$. Occasionally we have also injected total and/or size-fractionated rat kidney cortex poly(A)⁺ RNA (maximally 20 ng per oocyte). After 1–6 days, uptake of $^{35}\text{SO}_4^{2-}$, of methyl $\alpha\text{-D-}[^{14}\text{C}]\text{glucopyranoside}$, of L- $[^3\text{H}]\text{leucine}$, of $^{32}\text{P}_i$, and of L- $[^3\text{H}]\text{arginine}$ (New England Nuclear Radiochemicals) was measured in either the presence or absence of Na^+ , as described (15–20).

Isolation of RNA and mRNA. RNA was extracted (18, 19) from various tissues and, when specified, poly(A)⁺ RNA was isolated and size-fractionated by sucrose density gradient centrifugation (16, 18, 21).

Construction and Screening of a cDNA Library. A directional cDNA library was constructed by using size-selected rat kidney cortex poly(A)⁺ RNA that had been shown to maximally induce expression of Na^+ -dependent SO_4^{2-} transport activity in oocytes (2–3 kb; data not shown). The cDNA library was constructed by using a commercial kit (SuperScript plasmid system, pSPORT1 vector; GIBCO/BRL) following precisely as instructed by the supplier and contained about 2×10^5 colonies, of which 40,000 have been screened by a sib-selection procedure; initial pools for screening contained about 1000 colonies. Plasmid DNA was isolated by standard procedures (alkaline lysis and using Qiagen columns; Kontron, Zürich). Plasmids were linearized with *Not* I and used for *in vitro* synthesis of cRNA, including capping, with T7 RNA polymerase (Promega) (22). Synthesized cRNA was dissolved in water for further use.

DNA Sequencing/Primer Extension. Sequencing was carried out by the chain-termination method using a T7 polymerase sequencing kit (Pharmacia). Both strands of the cDNA insert have been sequenced. Synthetic oligonucleotides were used as primers to proceed through the entire sequence. To determine approximately the length of the 5' end of the NaSi-1 mRNA transcript, we used the Moloney murine leukemia virus reverse transcriptase RNase H⁻ primer extension system (Promega), following precisely the

The publication costs of this article were defrayed in part by page charge payment. This article must therefore be hereby marked "advertisement" in accordance with 18 U.S.C. §1734 solely to indicate this fact.

*To whom reprint requests should be addressed.

†The sequence reported in this paper has been deposited in the GenBank database (accession no. L19102).

supplier's protocol, with a 24-mer antisense oligonucleotide (5'-CGG-ATG-ATG-AGA-GGG-AGT-GGC-AAT-3') starting from position +92 on the NaSi-1 sequence. The oligonucleotide was labeled with [γ - 32 P]ATP and the extended products were analyzed by electrophoresis in a denaturing polyacrylamide gel (as specified by the Promega protocol for the primer extension system).

Northern Analysis. Total RNAs (≈ 30 μ g per lane) were denatured, electrophoresed in 1% agarose/formaldehyde gels and transferred to GeneScreen membranes (DuPont/NEN). cDNA probes of NaSi-1 (full length) and of mouse β -actin (1150-bp *Pst* I fragment; ref. 23) were labeled by random priming (Pharmacia) using [α - 32 P]dCTP (Amersham). Blots were prehybridized and hybridized in a buffer containing 5 \times SSPE (1 \times SSPE is 180 mM NaCl/10 mM NaPi, pH 7.4/1 mM EDTA), 1% SDS, 5 \times Denhardt's solution, herring sperm DNA (0.2 mg/ml), and 40% formamide, at 42°C overnight. Blots were washed four times in 2 \times standard saline citrate (SSC)/0.1% SDS at room temperature, then 20 min in 1 \times SSC/0.1% SDS at 50°C, followed by 20 min in 0.1 \times SSC/0.1% SDS at 60°C (high stringency), with the last step repeated if too much background radiation was present.

In Vitro Translation. NaSi-1 cRNA was translated with a rabbit reticulocyte lysate system in the absence or presence of canine pancreatic microsomes (Promega); we have followed the supplier's protocols with small modifications, as described (24).

RESULTS AND DISCUSSION

Similar to our previous studies on rabbit kidney cortex mRNA (17), injection of poly(A)⁺ RNA isolated from rat kidney cortex led to an expression of Na⁺-dependent SO₄²⁻ uptake in oocytes: 3- to 4-fold over intrinsic activity with total mRNA and 7- to 10-fold with size-fractionated mRNA (fractions containing 2-3 kb mRNA; injection of 15-20 ng, expression measured 3-4 days after injection; data not shown).

We constructed and screened a rat kidney cortex cDNA plasmid library by a sib-selection procedure on the basis of expression of Na⁺-dependent SO₄²⁻ transport in *X. laevis* oocytes. As shown in Fig. 1A, we obtained a single cDNA-

clone (NaSi-1) which specifically stimulated Na⁺-dependent SO₄²⁻ uptake. Injection of 1 ng of NaSi-1 cRNA led to >40-fold stimulation of SO₄²⁻ uptake (compared with intrinsic uptake in water-injected oocytes); no apparent stimulation of transport of methyl α -D-glucopyranoside, L-arginine, or L-leucine was observed (Fig. 1A). A weak stimulation of Na⁺/P_i cotransport was observed, which was subsequently shown to be insignificant (see below and Fig. 1B). The increase in SO₄²⁻ transport after injection of NaSi-1-cRNA was entirely Na⁺-dependent (Fig. 1A). Initial characterization of NaSi-1 cRNA-induced Na⁺-dependent SO₄²⁻ uptake documented that the magnitude of expression was related to the amount of cRNA injected (linear between 0.1 and 2.5 ng of cRNA per oocyte, with maximal stimulation between 5 and 20 ng of cRNA per oocyte; 1 day of expression; data not shown) and to the time of expression (up to 6 days, 1 ng of cRNA per oocyte injected; data not shown). Furthermore, under standard conditions (1-2 ng of cRNA injected; up to 4 days of expression) throughout the present study, Na⁺-dependent SO₄²⁻ transport was linear in the time of uptake (up to 60 min; data not shown).

Renal brush-border membrane Na⁺/SO₄²⁻ cotransport is a unique transport system which is distinct from Na⁺/P_i cotransport (see Introduction): Na⁺/SO₄²⁻ cotransport is not inhibited by P_i but is shared by thiosulfate. On the other hand, Na⁺/P_i cotransport is not inhibited by SO₄²⁻ (for review, see ref. 9); a cDNA encoding rat renal cortex Na⁺/P_i cotransport (NaPi-2) has been recently cloned (16). To further determine the selectivity of the presently cloned cotransport system (NaSi-1) and to distinguish it from the Na⁺/P_i cotransporter (NaPi-2), we injected oocytes with either NaSi-1 or NaPi-2 cRNA and studied SO₄²⁻ uptake or P_i uptake, respectively, and their mutual inhibition by either P_i, SO₄²⁻, or thiosulfate. NaSi-1 cRNA-induced SO₄²⁻ uptake was not inhibited by increasing P_i concentrations; as expected, it was inhibited by increasing concentrations of thiosulfate (Fig. 1B). NaPi-2 cRNA-induced P_i uptake was inhibited by P_i but not by SO₄²⁻ (Fig. 1C). Therefore, the data presented in Fig. 1 document that NaSi-1 cRNA stimulates with high potency a highly selective Na⁺/SO₄²⁻ cotransporter; i.e., at physiological concentrations of P_i and SO₄²⁻, this transporter will interact only

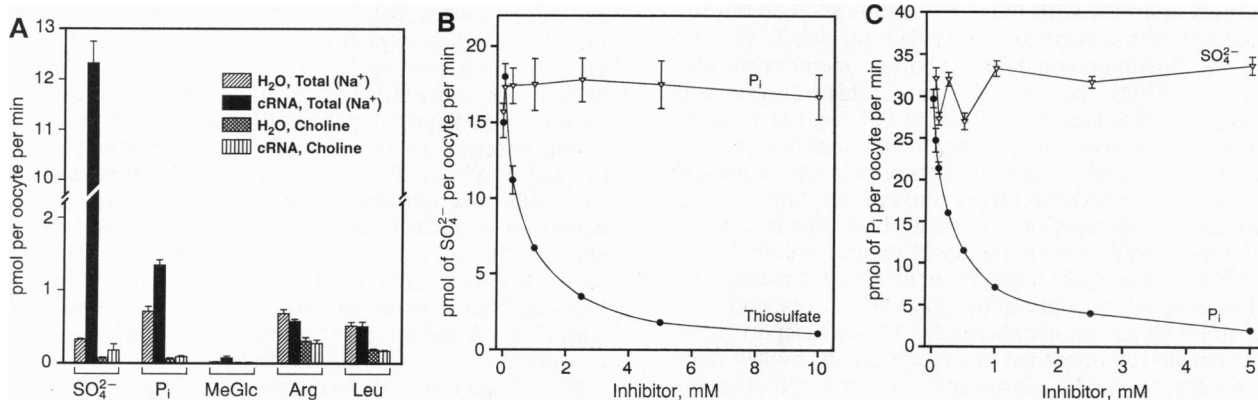


FIG. 1. Cloning of NaSi-1 cDNA and specificity of expressed uptake. (A) Oocytes were injected with 50 nl of water or 50 nl of NaSi-1 cRNA (1 ng per oocyte). One day after injection, transport was measured in the presence of Na⁺ (100 mM NaCl) and in its absence (100 mM choline chloride) with 0.5 mM K₂³⁵SO₄ (20-40 μ Ci/ml; 1 μ Ci = 37 kBq); 0.5 mM K₂H₃₁PO₄ (20-40 μ Ci/ml); 0.1 mM methyl α -D-[³H]glucopyranoside (12.5 μ Ci/ml); 50 μ M L-[³H]arginine (5 μ Ci/ml), and 50 μ M L-[³H]leucine (5 μ Ci/ml). Data are shown as means \pm SE for 7-10 oocytes per condition and are representative of at least two similar experiments. (B) Oocytes were injected with 50 nl of water or 50 nl of NaSi-1 cRNA (1 ng per oocyte). Two days after injection, transport was measured in a Na⁺ medium (100 mM NaCl) with 0.5 mM K₂³⁵SO₄ as substrate (20-40 μ Ci/ml) and various concentrations of thiosulfate (K₂S₂O₃, 0-10 mM) and P_i (K₂HPO₄, 0-10 mM) as inhibitors. Data are shown as means \pm SE for 7-10 oocytes per condition and are representative of at least two similar experiments. For thiosulfate, the inhibition constant (*K_i*) was calculated to be 0.33 mM. (C) Oocytes were injected with 50 nl of water or 50 nl of NaPi-2 cRNA (1 ng per oocyte; ref. 16). Two days after injection, transport was measured in a Na⁺ medium (100 mM NaCl) with 0.5 mM K₂HPO₄ as substrate (20-40 μ Ci/ml), and various concentrations of SO₄²⁻ (K₂SO₄, 0-5 mM) and P_i (K₂HPO₄, 0-5 mM) as inhibitors. Data are shown as means \pm SE for 7-10 oocytes per condition and are representative of at least two similar experiments. In Fig. 1, SE values not included were smaller than the symbols.

with SO_4^{2-} . However, as indicated by the slight stimulation of P_i transport in NaSi-1-injected oocytes (Fig. 1A), this transporter could also show a "weak" interaction with P_i when it is the only anion present.

To further characterize NaSi-1 cRNA-induced SO_4^{2-} uptake, we studied its Na^+ as well as SO_4^{2-} dependence (Fig. 2). SO_4^{2-} dependence showed simple Michaelis-Menten kinetics ($K_m = 0.62 \pm 0.08$ mM; Fig. 2A). For the Na^+ interaction of NaSi-1 cRNA-induced transport, a sigmoidal relationship was observed (Fig. 2B); these data were fitted to a generalized Hill equation ($K_m = 16.8 \pm 2.9$ mM; Hill coefficient $n = 1.8 \pm 0.4$). The above properties of NaSi-1-induced Na^+ -dependent SO_4^{2-} uptake (Fig. 1A and B; Fig. 2A and B) are in close agreement with the properties of brush-border vesicle $\text{Na}^+/\text{SO}_4^{2-}$ cotransport (e.g., refs. 3, 5, and 7; for review, see ref. 1).

4,4'-Diisothiocyanatostilbene-2,2'-disulfonate (DIDS) is a known anion-exchange inhibitor that inhibits Na^+ -independent SO_4^{2-} transport in rat renal cortex basolateral membranes (4). We observed no effect of DIDS (up to 1 mM) on the NaSi-1-induced $\text{Na}^+/\text{SO}_4^{2-}$ cotransport activity (data not shown), confirming that NaSi-1 encodes a Na^+ -coupled transport system (and not an anion exchanger).

By Northern blot hybridization using full-length NaSi-1 cDNA as a probe, we analyzed tissue/organ distribution in the rat, and species homologies with kidney cortical tissues of various mammalian species. In RNAs from various rat tissues (Fig. 3), two transcripts (2.3 and 2.9 kb) were detected in kidney cortex, kidney medulla/papilla, upper small intestine (duodenum and jejunum) and lower small intestine (ileum). With β -actin as an internal standard, the hybridization signals were stronger in kidney cortex than in kidney medulla/papilla and stronger in lower small intestine (ileum) than in upper small intestine (duodenum and jejunum; Fig. 3). No hybridization signals were observed in RNA from other rat tissues (proximal colon, lung, liver, brain, heart, and skeletal muscle; Fig. 3 and data not shown). The above distribution of NaSi-1 related mRNA(s) is in agreement with

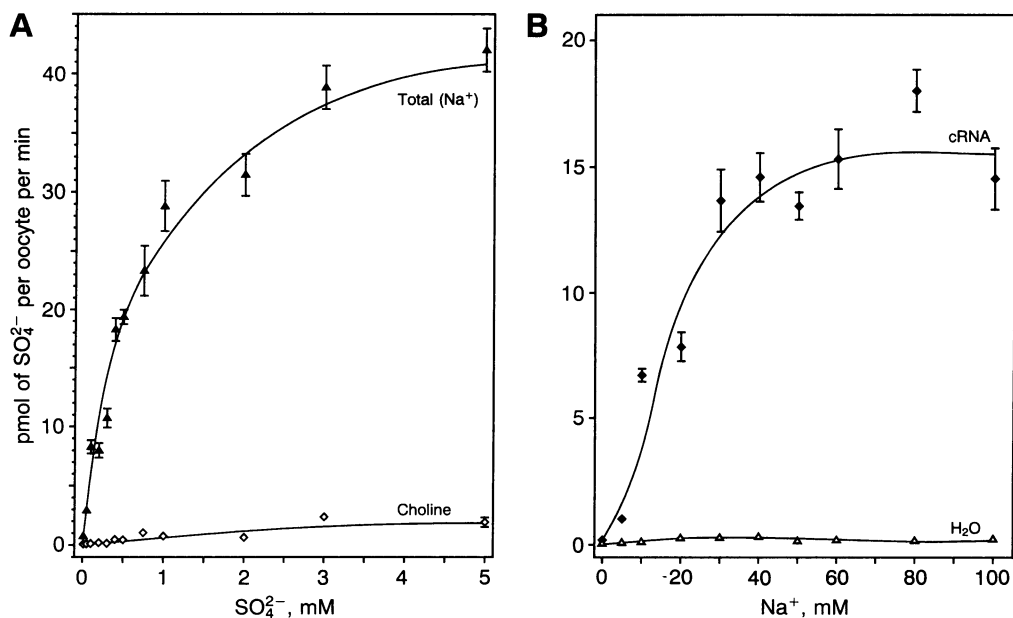


FIG. 2. Na^+ and SO_4^{2-} concentration dependence of NaSi-1 cRNA-induced SO_4^{2-} uptake. (A) Oocytes were injected with 50 nl water or 50 nl NaSi-1 cRNA (1 ng per oocyte). Two days later, transport was measured in the presence of Na^+ (100 mM NaCl; \blacktriangle) and in its absence (100 mM choline chloride; \diamond) with 0.01–5.0 mM K_2SO_4 as substrate (20–40 $\mu\text{Ci}/\text{ml}$). Data are shown as means \pm SE for 7–10 oocytes per condition, and are representative of four similar experiments. The curve was fitted to a Michaelis-Menten equation by nonlinear regression ($K_m = 0.62 \pm 0.08$ mM; $V_{\text{max}} = 42.7 \pm 2.0$ pmol/min). (B) Oocytes were injected with 50 nl of water (\triangle) or 50 nl of NaSi-1 cRNA (1 ng per oocyte; \blacklozenge). Two days later, transport was measured in the presence of various concentrations of Na^+ (0–100 mM NaCl; isoosmotically replaced by choline chloride) with 0.5 mM K_2SO_4 (20–40 $\mu\text{Ci}/\text{ml}$). Data are shown as means \pm SE for 7–10 oocytes per condition and are representative of three similar experiments. The curve was fitted to a generalized Hill equation by nonlinear regression ($K_m/K_D = 16.8 \pm 2.9$ mM; apparent $V_{\text{max}} = 17.0 \pm 1.4$ pmol/min; $n = 1.8 \pm 0.4$). SE bars not visible were smaller than the symbols.

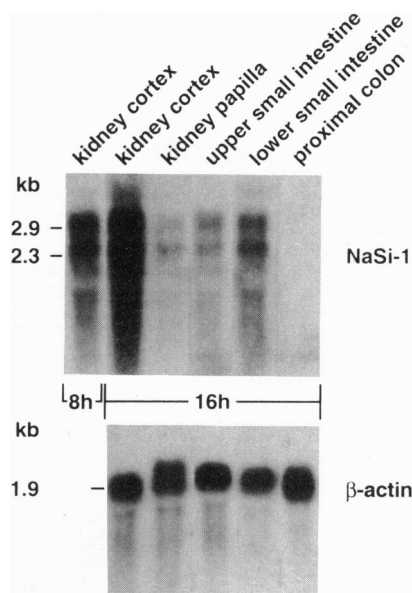


FIG. 3. Northern blot hybridization using full-length NaSi-1 and partial length β -actin cDNA probes. Total RNA samples from various rat tissues were analyzed with an NaSi-1 cDNA probe. Hybridization signals (2.3 kb and 2.9 kb) were observed only with kidney cortex, kidney medulla/papilla, upper small intestine (duodenum and jejunum) and lower small intestine (ileum). The β -actin signals obtained from the same blots are given to provide information on the quality and amount of samples loaded. For kidney cortex, two different exposure times (8 and 16 hr) are given for visualization of the two bands.

NaSi-1 being related to brush-border membrane $\text{Na}^+/\text{SO}_4^{2-}$ cotransport. Cross-species hybridization of NaSi-1 was observed with kidney cortex RNAs from mouse (2.3 and 2.6 kb), rabbit (2.6 and 3.3 kb), and pig (3.2 kb) (data not shown),

-17 5'-CC CAC GCG TCC GGG ACA

1	ATG AAG CTC CTC AAT TAC GCT TTT GTG TAT CGT CGC TTT CTC CTT GTG GTT TTC	1027	ATG AGG TAT CAA GAA ATC GTG ACC TTG GTG ATC TTC ATT GTA ATG GCC TTG CTC
1	Met Lys Leu Leu Asn Tyr Ala Phe Val Tyr Arg Arg Phe Leu Leu Val Val Phe	343	Met Arg Tyr Gln Glu Ile Val Thr Leu Val Ile Phe Ile Val Met Ala Leu Leu
			M 5
55	ACT GTT TTG GTT TTA TTG CCA CTC CCT CTC ATC ATC CGT AGC AAG GAA GCA GAA	1081	TGG TTC AGT CCG GAC CCT GGC TTT GTC ACT GGT TGG TCA GTC CTG TTT TCA GAG
19	Thr Val Leu Val Leu Leu Pro Leu Pro Leu Ile Ile Arg Ser Lys Glu Ala Glu	361	Trp Phe Ser Arg Asp Pro Gly Phe Val Thr Gly Trp Ser Val Leu Phe Ser Glu
	M 1		
109	TGT GCC TAC ATC CTC TTT GTT ATT GCC ACA TTT TGG ATC ACA GAA GCC TTG CCC	1135	TAC CCG GGT TAT GTT ACA GAT TCA ACT GTT GCC TTA GTT GCA GGA ATC CTT TTC
37	Cys Ala Tyr Ile Leu Phe Val Ile Ala Thr Phe Thr Ile Thr Glu Ala Leu Pro	379	Tyr Pro Gly Tyr Val Thr Asp Ser Thr Val Ala Leu Ala Glu Ile Leu Phe
	M 2		M 6
163	CTG TCA ATC ACA GCT CTA CTG CCT GGG TTA ATG TTC CCC ATG TTT GGA ATC ATG	1189	TTT CTA ATT CCA GCC AAG AAA CTG ACA AAA ATG ACA TCC ACA GGA GAT ATT ATT
55	Leu Ser Ile Thr Ala Leu Leu Pro Gly Leu Met Phe Pro Met Phe Gly Ile Met	397	Phe Leu Ile Pro Ala Lys Lys Leu Thr O Lys Met Thr Ser Thr Gly Asp Ile Ile
	M 2		
217	TCT TCT ACA CAT GTA GCT TCT GCT TAC TTC AAA GAC TTT CAC CTT CTG CTA ATT	1243	GCT TTT GAT TAT TCT CCC CTG ATT ACT TGG AAA GAA TTC CAG TCA TTC ATG CCC
73	Ser Ser Thr His Val Ala Ser Ala Tyr Phe Lys Asp Phe His Leu Leu Leu Ile	415	Ala Phe Asp Tyr Ser Pro Leu Ile Thr Trp Lys Glu Phe Gln Ser Phe Met Pro
			●
271	GGA GTC ATC TGC TTA GCA ACA TCA ATA GAA AAA TGG AAT TTG CAC AAG AGG ATT	1297	TGG GAC ATA GCC ATT CTC GTT GGT GGA GGC TTT GCA CTG GCA GAT GGT TGT CAG
91	Gly Val Ile Cys Leu Ala Thr Ser Ile Glu Lys Trp Asn Leu His Lys Arg Ile	433	Trp Asp Ile Ala Gln Leu Val Gly Ile Leu Val Glu Gly Ile Leu Leu Pro Ser Thr Leu Cys
	M 3		
325	GCT CTG AGG ATG GTG ATG ATG GTG GGG GTG AAT CCG GCC TGG CTG ACG TTG GGG	1351	GTA TCA GGA CTA TCT AGC TGG ATA GGA AGT AAA TTA TCT CCT TTA GGT TCG TTA
109	Ala Leu Arg Met Val Leu Met Val Gly Val Asn Pro Ala Trp Leu Thr Leu Gly	451	Val Ser Gly Leu Ser Ser Trp Ile Gly Ser Lys Leu Ser Pro Leu Gly Ser Leu
379	TTC ATG AGC AGT ACT GCC TTC TTA TCT ATG TGG CTT AGC AAC ACC TCT ACT GCT	1405	CCA GTT TGG CTA ATA ATT CTG ATA TCC TCT TTG ATT GTC ACA TCT TTG ACA GAG
127	Phe Met Ser Ser Thr Ala Phe Leu Ser Met Trp Leu Ser Asn Thr Ser Thr Ala	469	Pro Val Trp Leu Ile Ile Leu Ile Ser Ser Leu Ile Val Thr Ser Leu Thr Glu
	M 3		M 7
433	GCC ATG GTG ATG CCC ATC GTG GAG GCA GTG GCG CAG CAG ATC ACC AGT GCT GAA	1459	GTA GCC AGC AAC CCA GCT ACC ATT ACC ATT CTG TTC CCC ATA TTA TCT CCT TTG
145	Ala Met Val Met Pro Ile Val Glu Ala Val Ala Gln Gln Ile Thr Ser Ala Glu	487	Val Ala Ser Asn Pro Ala Thr Ile Thr Ile Leu Phe Pro Ile Leu Ser Pro Leu
487	GCA GAG GCC GAG GCC ACT CAG ATG ACT TAT TTC AAT GAA TCT GCC GCC CAG GGA	1513	GCT GAA GCC ATT CAT GTG AAC CCT CTT CAC ATT TTG CTG CCA TCC ACA CTT TGT
163	Ala Glu Ala Glu Leu Thr Tyr Phe Asn Glu Thr Tyr Phe Asn Glu Thr Ser Ala Ala Gln Gly	505	Ala Glu Ala Ile His Val Asn Pro Leu His Ile Leu Leu Pro Ser Thr Leu Cys
	⊙		
541	CTC GAA GTT GAT GAA ACT ATT ATT GGA CAA GAA ACA AAT GAG AGG AAA GAG AAA	1567	ACC TCA TTT GCA TTT CTC CTG CCA GTT GCA AAT CCA CCC AAT GCC ATT GTG TTT
181	Leu Glu Val Asp Glu Thr Ile Ile Gly Gln Glu Thr Asn Glu Arg Lys Glu Lys	523	Thr Ser Phe Ala Phe Leu Leu Pro Val Ala Asn Pro Pro Asn Ala Ile Val Phe
595	ACA AAA CCA GCT CTA GGA AGC AGT AAT GAC AAA GGG AAA GTG TCA AGC AAG ATG	1621	TCA TAT GGC CAC CTG AAA GTC ATT GAC ATG GTT AAA GCT GGA CTC GGA GTA AAC
199	Thr Lys Pro Ala Leu Gly Ser Ser Asn Asp Lys Gly Lys Val Ser Ser Lys Met	541	Ser Tyr Gly His Leu Lys Val Ile Asp Met Val Lys Ala Gly Leu Gly Val Asn
649	GAG ACA GAA AAG AAC ACA GTC ACA GGA GCA AAG TAT CCG TCA AAG AAG GAC CAC	1675	ATT TTG GGT GTT GCT GTG GTG ATG CTG GGC ATG TTC ACC TGG ATC GAA CCT ATG
217	Phe Pro Val Ala Val Ile Leu Leu Leu Leu Ser Trp Ile Trp Lys Lys Asp His	559	Ile Leu Gly Val Ala Val Val Met Leu Gly Met Phe Thr Trp Ile Glu Pro Met
			M 8
703	ATG ATG TGT AAG CTC ATG TGT TTA TGT ATT GCT TAC TCT TCA ACC ATT GGT GGA	1729	TTT AAC CTC CAC GAA TAT CCC TCC TGG GCT CCT GAC ATT GTT AAT CAG ACC ATG
235	Met Met Cys Lys Leu Met Cys Leu Cys Ile Ala Tyr Ser Ser Thr Ile Gly Gly	577	Phe Asn Leu His Glu Tyr Pro Ser Trp Ala Pro Asp Ile Val Asn Gln Thr Met
757	CTG ACG ACA ATC ACT GGT ACC TCC ACC AAC CTG ATC TTC TCC GAG CAT TTC AAC	1783	CCA TGA CAC ACA CAC AAG AGC TAC CAG TTT GCG GTG GCT TCA GGA CTC GCT AAG
253	Leu Thr Thr Ile Thr Gly Thr Ser Thr Asn Leu Ile Phe Ser Glu His Phe Asn	595	Pro ***
811	ACA CGC TAC CCT GAT TGT CGC TGC CTC AAC TTT GGA TCT TGG TTT TTG TTT TCC	1837	AAT GAC TGT ACG GTA CAG CCG GAT TGG ACT GGC ACA CGC GAA TCT TCG ATG CAG
271	Thr Arg Tyr Pro Asp Cys Arg Cys Leu Asn Phe Gly Ser Trp Phe Leu Phe Ser	1891	CTA TTC CAA TTG CAG AGC GTG CCC CAC ACA TGC CCC TGT CAA CCT CAT AAG ACA
865	TTC CCG GTC GCT GTT ATT CTT CTA CTT TTG TCT TGG ATT TGG CTT CAA TGG CTT	1945	GAG TTC ATA TCT TTT GAA ATA CAA TCA ACG TGC ATC TAC CCG CCT TCG TCC AAA
289	Phe Pro Val Ala Val Ile Leu Leu Leu Leu Ser Trp Ile Trp Lys Lys Asp His	1999	AAT CAG GTT GAG ACG CAT CGC AGA CCA GCT ACA TGC TCT TTG TCC ATT ATA ATG
	M 4		
919	TTC TTA GGA TTC AAC TTT AAG GAG ATG TTC AAG TGT GGC AAA ACC AAA ACA CTC	2053	ACA CTT AAG GAC CTT CAA AAA AGT TAG GCC ATC CGT CCG TCG CAT CTT AAA TTC
307	Phe Leu Gly Phe Asn Phe Lys Glu Met Phe Lys Cys Gly Lys Thr Lys Thr Leu	2107	GGA GTT CAT TGG GAC ATT TCA AAC ATC AAT TCA CTA TTT GAA ATT TTT TTT ATG
			●
973	AAA GAA AAA GCT TGT GCC GAG GTG ATC AAG CAA GAA TAT GAA AAA CTT GGG CCA	2161	AAA CTA AAG GCA GAA AAT AAA GTG TGA AAG TAA ACG AGA AAAAAAAAAAAAAAAAAA
325	Lys Glu Lys Ala Cys Ala Glu Val Ile Lys Gln Glu Tyr Glu Lys Leu Gly Pro	2219	AAAA - 3'

Fig. 4. Nucleotide and predicted amino acid sequence of NaSi-1 cDNA. Nucleotides are numbered beginning with the first ATG initiation codon within a strong Kozak consensus sequence (25); the stop codon (TGA) is indicated by stars. Putative transmembrane domains (M1–M8) are underlined. Potential N-glycosylation sites (aa 140 and 174) are indicated by circled stars; potential phosphorylation sites located at the cytoplasmic surface are labeled (○, protein kinase A; ●, protein kinase C). An additional putative N-glycosylation site is at aa 591 and other potential phosphorylation sites are at aa 213, 218, and 230 for protein kinase C and at position 39 for tyrosine kinase. The polyadenylation signal preceding the poly(A) tail is doubly underlined.

suggesting that the NaSi-1 transcript may be highly homologous to the corresponding transcripts ($\text{Na}^+/\text{SO}_4^{2-}$ cotransporters) in other species.

The NaSi-1 cDNA insert was completely sequenced on both strands (Fig. 4). It is 2239 bp long, with 17 nt prior to the first start codon (ATG) and a stop codon (TGA) at position 1786. Thereafter, another 434 nt are present at the 3' end, with a putative polyadenylation signal (AATAAA) at position 2176, closely followed by a 24-nt poly(A) tail. The predicted open reading frame is 595 aa long, which corresponds to a protein of 66 kDa (Fig. 4). Due to a potential signal cleavage site at aa 33 (after the first hydrophobic domain; Figs. 4 and 5), the mature protein might differ in size.

To approximately determine whether the cloned NaSi-1 cDNA corresponds to the 2.3-kb mRNA band seen in Northern blots, we performed a primer extension experiment using rat kidney cortex mRNA and an antisense primer starting at nt +92 (see *Experimental Procedures*). The extended product, analyzed in a polyacrylamide gel, was about 110 bp long (data not shown), which is in agreement with the length of the 5' end of the cloned NaSi-1 cDNA. We therefore believe that the NaSi-1 cDNA corresponds in length to the 2.3-kb mRNA seen in Northern blots (Fig. 3). We also assume that the

2.9-kb mRNA (Fig. 3) is closely related to NaSi-1 and might represent an mRNA with a prolonged 3' untranslated region

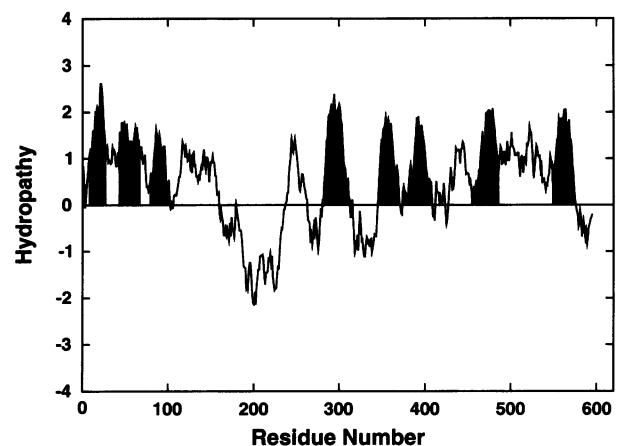


Fig. 5. Hydropathy analysis of the deduced NaSi-1 amino acid sequence by the algorithm of Kyte and Doolittle (26) with a window of 17. Shaded areas show eight putative transmembrane domains.

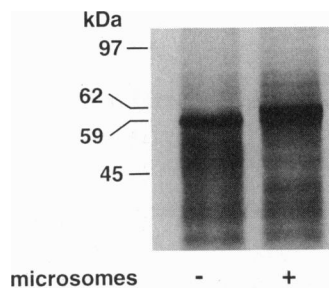


FIG. 6. *In vitro* translation of NaSi-1 cRNA. One microgram of NaSi-1 cRNA was used and the translation products were analyzed directly by SDS/10% PAGE. In the absence of microsomes, the major translation product has an average size of 59 kDa; in the presence of microsomes the major translation product is shifted to 62 kDa, indicating some core glycosylation.

(e.g., due to the use of a different polyadenylation site; see ref. 24).

In vitro translation of NaSi-1 cRNA with rabbit reticulocyte lysate resulted in a major band of 59 kDa, which was shifted to 62 kDa in the presence of microsomes (Fig. 6), suggesting that under these conditions, core glycosylation at only one of the three putative N-glycosylation sites may occur (Fig. 4). Comparison of the deduced amino acid sequence of NaSi-1 against Swiss-Prot and Protein Identification Resource databases (confirmed on July 23, 1993 by using the BLAST network) revealed no significant overall similarities, especially not to other cloned Na⁺/solute cotransport systems. Notably, a conserved region (SOB motif; refs. 14 and 27) found in certain Na⁺-dependent mammalian [e.g., SGLT1 family (14, 28) and Na/P_i cotransporters (15, 16)] and nonmammalian cotransport systems (27) is absent in NaSi-1. Hydrophobicity analysis of the deduced amino acid sequence (26, 29) suggests at least eight membrane-spanning domains (Fig. 5) with a cytoplasmic location of both termini and a large putative hydrophilic extracellular loop containing two potential N-glycosylation sites, Asn¹⁴⁰ and Asn¹⁷⁴ (Fig. 4). In the suggested secondary model of NaSi-1, three potential phosphorylation sites (Thr⁴⁰⁵ for protein kinase A and Thr³²³ and Thr⁴²³ for protein kinase C) are present at the cytoplasmic surface (Fig. 4).

Based on the above data, we conclude that we have cloned a rat cDNA closely related to proximal-tubular (and small-intestinal) brush-border membrane Na⁺/SO₄²⁻ cotransport; tissue distribution and the characteristics of expressed uptake are in support of this conclusion. The NaSi-1-encoded protein does not show significant homologies to other cloned Na⁺/solute cotransport systems. The cloning of a probable brush-border membrane Na⁺/SO₄²⁻ cotransporter represents a significant step toward the cellular/molecular understanding of renal/small-intestinal Na⁺-dependent solute reabsorption. In addition to providing primary structural information, NaSi-1 may be an invaluable experimental tool for further studies on the physiological regulation of small-intestinal and renal proximal-tubular Na⁺/SO₄²⁻ cotransport.

We thank D. Rossi and C. Gasser for their help in preparing the manuscript. This work was supported by a Grant 32.30785.91 of the Swiss National Science Foundation.

- Murer, H., Manganel, M. & Roch-Roch-Ramel, F. (1992) *Handbook of Physiology, Renal Section 8. Vol. II*, ed. Windhager, E. (Oxford Univ. Press, Oxford, UK), Chap. 47, pp. 2165–2188.
- David, C. & Ullrich, K. J. (1992) *Pfluegers Arch.* **421**, 455–465.
- Ahearn, G. A. & Murer, H. (1984) *J. Membr. Biol.* **78**, 177–186.
- Baestlein, C. & Burckhardt, G. (1986) *Am. J. Physiol.* **250**, F226–F234.
- Luecke, H., Stange, G. & Murer, H. (1979) *Biochem. J.* **182**, 223–229.
- Schneider, G. E., Durham, J. C. & Sacktor, B. (1984) *J. Biol. Chem.* **259**, 14591–14599.
- Turner, R. J. (1984) *Am. J. Physiol.* **247**, F793–F798.
- Pajfro, J. L., Clark, N. B., Metts, R. E. & Lynch, M. A. (1989) *Am. J. Physiol.* **256**, R1176–R1183.
- Murer, H. (1992) *J. Am. Soc. Nephrol.* **2**, 1649–1665.
- Tenenhouse, H. S., Lee, J. & Harvey, N. (1991) *Am. J. Physiol.* **261**, F420–F426.
- Neiberger, R. & Gomez, P. (1992) *J. Am. Soc. Nephrol.* **3**, 66P (abstr.).
- Tallgren, L. G. (1980) *Acta Med. Scand. Suppl.* **640**, 1–100.
- Pajor, A. M., Hirayama, B. A. & Wright, E. M. (1992) *Biochim. Biophys. Acta* **1106**, 216–220.
- Wright, E. M., Hager, K. M. & Turk, E. (1992) *Curr. Opin. Cell Biol.* **4**, 696–702.
- Werner, A., Moore, M. L., Mantei, N., Biber, J., Semenza, G. & Murer, H. (1991) *Proc. Natl. Acad. Sci. USA* **88**, 9608–9612.
- Magagnin, S., Werner, A., Markovich, D., Sorribas, V., Stange, G., Biber, J. & Murer, H. (1993) *Proc. Natl. Acad. Sci. USA* **90**, 5979–5983.
- Werner, A., Biber, J., Forgo, J., Palacin, M. & Murer, H. (1990) *J. Biol. Chem.* **265**, 12331–12336.
- Bertran, J., Werner, A., Stange, G., Markovich, D., Biber, J., Testar, X., Zorzano, A., Palacin, M. & Murer, H. (1992) *Biochem. J.* **281**, 717–723.
- Bertran, J., Werner, A., Moore, M. L., Stange, G., Markovich, D., Biber, J., Testar, X., Zorzano, A., Palacin, M. & Murer, H. (1992) *Proc. Natl. Acad. Sci. USA* **89**, 5601–5605.
- Bertran, J., Magagnin, S., Werner, A., Markovich, D., Biber, J., Testar, X., Zorzano, A., Kühn, L. C., Palacin, M. & Murer, H. (1992) *Proc. Natl. Acad. Sci. USA* **89**, 5606–5610.
- Magagnin, S., Bertran, J., Werner, A., Markovich, D., Biber, J., Palacin, M. & Murer, H. (1992) *J. Biol. Chem.* **267**, 15384–15390.
- Short, J. M., Fernandez, J. M., Sorge, J. A. & Huse, W. D. (1988) *Nucleic Acids Res.* **16**, 7583–7600.
- Alonso, S., Minty, A., Bourlet, J. & Buckingham, M. (1986) *Mol. Evol.* **23**, 11–22.
- Markovich, D., Stange, G., Bertran, J., Palacin, M., Werner, A., Biber, J. & Murer, H. (1993) *J. Biol. Chem.* **268**, 1362–1367.
- Kozak, M. (1989) *J. Cell Biol.* **108**, 229–241.
- Kyte, J. & Doolittle, R. F. (1982) *J. Mol. Biol.* **157**, 105–132.
- Deguchi, Y., Yamato, I. & Anraku, Y. (1990) *J. Biol. Chem.* **265**, 21704–21708.
- Kong, C.-T., Yet, S.-F. & Lever, J. E. (1993) *J. Biol. Chem.* **268**, 1509–1512.
- Klein, P., Kanehisa, M. & DeLisi, C. (1985) *Biochim. Biophys. Acta* **815**, 468–476.